A Minimal Cost Path and Level Set Evolution Approach for Carotid Bifurcation Segmentation

Release 0.00

Karl Krissian[1], Sara Arencibia García[1]

July 21, 2009

[1]University of Las Palmas of Gran Canaria, Las Palmas, Spain

Abstract

We propose a new approach for semi-automatic segmentation of the carotid bifurcation as part of the Carotid Lumen Segmentation and Stenosis Grading Challenge MICCAI'2009 workshop. Three initial points are provided as input, belonging to the Common, the External and the Internal Carotid Arteries. Our algorithm is divided into two main steps: first, two minimal cost paths are tracked between the CCA and both the ECA and the ICA. The cost functions are based on a multiscale vesselness response. Second, after detecting the junction position and cutting or extending the paths based on the requested lengths, a level set segmentation is initialized as a thin tube around the computed paths and evolves until reaching the vessel wall or a maximal evolution time. Results on training and testing datasets are presented and compared to the manual segmentation by three observers, based on a ground truth and using four quality measures.

Latest version available at the Insight Journal [http://hdl.handle.net/10380/xxx]

Contents

1 Introduction

In the context of the Carotid Lumen Segmentation and Stenosis Grading Challenge (CLS), forming part of the 3rd MICCAI Worshop in the series "3D Segmentation in the Clinic: a Grand Challenge", we propose a method for semi-automatic segmentation of the carotid bifurcation from Computed Tomography Angiography (CTA) datasets. The region to be segmented consists in parts of the Common Carotid Artery (CCA), the Internal Carotid Artery (ICA) and the External Carotid Artery (ECA), as defined by the challenge rules. The semi-automatic method challenge consists in using three points as input, each point located in one of the main arteries. Figure 1 depicts a volume rendering of datasets 000 and 004 [1]. The left column renders a volume of interest, and right column renders only the voxels belonging or close to the given segmentation ground truth. From these two images, we can understand most of the difficulties that can arise during the segmentation process:

- the presence of strong calcifications both in the ECA and the ICA,
- the presence of ramifications in the ECA,
- other unwanted vessels that come close to the main carotid arteries,
- the possibility of having a full obstruction of the ICA,
- a strong variation of vessel intensities between datasets and within the same dataset.

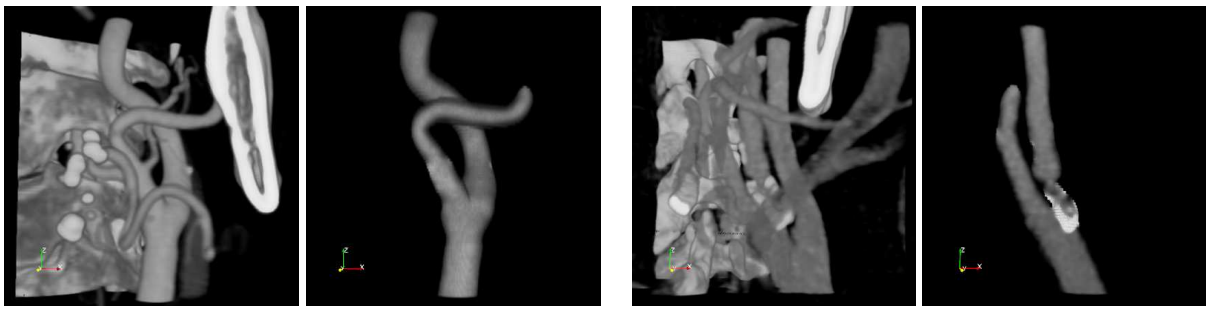

Figure 1: Volume Rendering of regions of interest from two datasets. From left to right, for dataset 000: volume rendering of the entire region of interest and of the voxels close to the given ground truth, for dataset 004: the same representation.

Based on the three initial points given within the semi-automatic challenge, we propose to use the strategy illustrated in figure 2 to segment the carotid bifurcation. This strategy is composed of the following main steps:

1. Compute the paths between the point in the CCA and the two other points.

[1] Rendered with ParaView http://www.paraview.org/ .

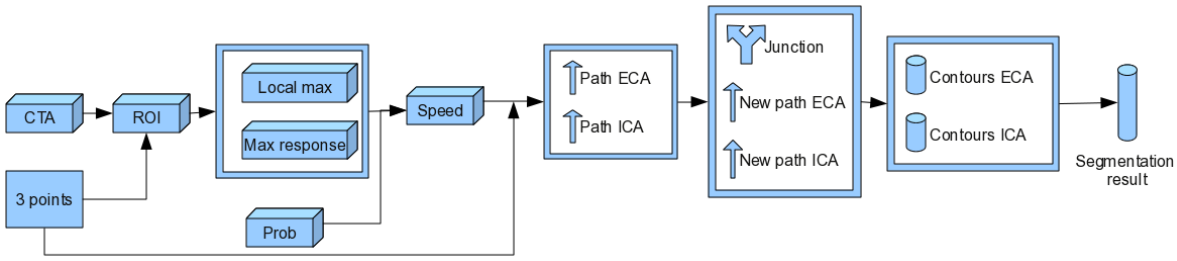

Figure 2: Main components of the proposed segmentation method.

2. Estimate the position of the junction, identify the two paths and adjust their length.

3. Segment the vessels starting from a thin tube around the paths and using a level set framework.

We details each step in the following sections, then we present and discuss the results obtained on the different datasets and we conclude.

2 Paths and Junction Computation

To start with, a region of interest is created based on the three given points, and using a margin of 30mm in X and Y, a bottom margin of 20mm in Z and a top margin of 40mm in Z direction. Creating the region of interest allows reducing the overall computation time before the detection of the junction location. Within this ROI, a speed image is created by combining the results of a multiscale vesselness measure and probability image based on the image intensity local statistics. Based on the speed image, a path for between the CCA and each of the other two arteries is created, allowing to identify a junction position and to which artery each path belongs to. The length of each path is either cut or extended to fulfill the requirements of the challenge. The different algorithms are described below.

2.1 Multiscale Vesselness Measure

A vesselness response is calculated based on [6] and similarly to [3]. The response is calculated using the input ROI. In addition, the algorithm has the following inputs: input image, minimal radius, maximal radius, number of radii and mask image.

Mask image

A mask image is created to reduce the total computation cost of the algorithm, the mask consist in a selection of voxels within the intensity range of vessels, this range has been set to $[1150, 1600]$ for all the datasets.

Local structure orientation

For describing the local structure orientation, we use the same second order descriptor as presented in [2, 4, 5]. It consists in a combination of the outer product of the gradient and the squared Hessian matrix, weighted by a coefficient β, as defined by (1). The derivatives are obtained by convolution with the corresponding

derivatives of a Gaussian kernel of standard deviation σ, and they are normalized using a multiplication by a factor σ^n, where n is the order of derivation, thus ensuring the scale invariance property which allows comparing responses obtained from different scales. This new operator will be denoted as $D_\sigma(I)$ and defines a local matrix at each voxel of the image, which is symmetric, real, and positive-semi definite,

$$D(I) = \nabla I \otimes \nabla I + \beta H^2(I), \quad (1)$$

$$D_\sigma(I) = \sigma^2 \nabla_\sigma I \otimes \nabla_\sigma I + \beta \sigma^4 H^2_\sigma(I). \quad (2)$$

At each voxel, we denote $\vec{\mathbf{v}}_1, \vec{\mathbf{v}}_2$ and $\vec{\mathbf{v}}_3$ the eigenvectors of $D_\sigma(I)$ with the respective eigenvalues $\lambda_1 \geq \lambda_2 \geq \lambda_3$. For the smallest eigenvalue, the eigenvector $\vec{\mathbf{v}}_3$ gives the local direction of minimal change, which, in the case of vessels, corresponds to the local orientation of the vessel axis. In all the experiments, we set the value of β to 1.

Circle boundary integration

For each scale σ, a response is computed as a combination of the boundary information along a circle in the estimated cross-section plane of the vessel. The *circle* $C_{\mathbf{x},\vec{\mathbf{v}}_1,\vec{\mathbf{v}}_2,\tau\sigma}$ is defined by its center $\mathbf{x}$, an estimate of the cross-section orientation given by the eigenvectors $\vec{\mathbf{v}}_1$ and $\vec{\mathbf{v}}_2$, and a radius proportional of the current scale $\tau\sigma$.

The *boundary information*, denoted B, is obtained with the scalar product of the gradient and the radial direction. An initial version of this filter consisted in averaging the boundary values around the computed circle:

$$M_\sigma(\mathbf{x}) = mean_{\mathbf{y}\in C} B(\mathbf{y}) = \frac{1}{N} \sum_{i=0}^{N-1} -\sigma \nabla_\sigma I\,(\mathbf{x} + \tau\sigma\,\vec{\mathbf{v}}_\alpha)\,.\vec{\mathbf{v}}_\alpha, \quad (3)$$

with $\alpha = 2\pi i/N$, and $\vec{\mathbf{v}}_\alpha = cos(\alpha)\vec{\mathbf{v}}_1 + sin(\alpha)\vec{\mathbf{v}}_2$, where N is the number of points along the circle. In all the experiments, the value τ is set to $\sqrt{3}$, to maximize the selected response at the center in the case of a cylindrical circular vessel with Gaussian cross-section [6], and the number of points N around the integrating circle is set to 20.

In order to improve both the selectivity of the filter and its robustness to outliers, we introduce the modifications:

1. we only keep the minimum of the boundary information in opposite directions,
2. we select the average over 80% of the highest obtained values.

The first modification allows reducing the response obtained at standard edges, where high gradients are present in only one side of the circle. The second modification prevents strong reduction of the vesselness response in the presence of junctions or similar intensity nearby structures.

Multiscale integration

We compute the response function M_σ for a range of scales that are discretized using a logarithmic scale in order to have more accuracy for lower scales. The minimal and maximal radius of the vessels to extract are set to 0.2 and 3.5mm respectively. The corresponding scales are calculated based on the relation between

the radius r of the cylindrical circular model and the scale $\sigma(r)$ at which it gives a maximal response at the center [6]:

$$\sigma(r) = \frac{\sqrt{2}}{2} r \tag{4}$$

We have set the number of scales to 7 from 0.5mm to 7mm for all experiments.

Two images are obtained as output of the multiscale vesselness filter:

1. The maximal response obtained across the different scales, denoted $M_{rep} = \max_\sigma M_\sigma$.
2. The image of the local maxima, denoted M_{lmax}, both in the spatial and the scale dimensions, of the multiscale response. A voxel is defined to be a local maxima of the multiscale response if and only if: - there exists a scale for which it is a local maximum of the response in the estimated plane of the cross-section, and - its response values at the previous and the next scales are lower.

The image of local maxima is an estimate of the vessel centerlines and will be used in the subsequent process to defined the cost associated to crossing a voxel (or equivalently the evolution speed), in order to find the centerline paths of the arteries. Figure 3 depicts the two output images obtained for datasets 000 and 004, where the rendering is obtained by Maximal Intensity Projection with fog effect to attenuate object depending on their distance to the camera [2].

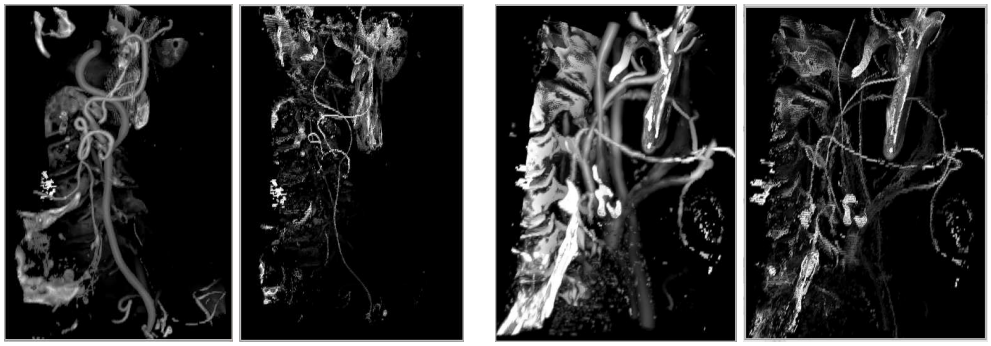

Figure 3: Maximum Intensity Projection (MIP) rendering of vesselness response and the corresponding local maxima from two datasets. From left to right, for dataset 000: MIP with OpenGL fog effect for the vesselness response and the local maxima images, for dataset 004: the same representation.

2.2 Probability and Speed Image Calculation

Since the regions of interest can contain many tubular structures that do not necessarily belong to the main carotid arteries, and since the vesselness response is sensitive to the presence of calcifications, we use an additional image based on local intensity statistics to create the speed image used for minimal cost path computation. Two images of local mean intensity, denoted I_{lm} and of local intensity standard deviation, denoted I_{sdm}, using neighborhoods of size $3 \times 3 \times 3$, are created. Based on these two image, a new image is created, denoted as probability image, using the expression:

$$I_p = f(I_{lm}) * g(I_{sdm}), \tag{5}$$

[2] Rendered with AMILab http://amilab.sourceforge.net/ .

where f is a smoothed version of an function which equals 1 within the intensity range $[1050, 1600]$ and 0 elsewhere, and g is defined by the expression $g(x) = e^{-\frac{x^2}{2.30^2}}$.

The speed image is then defined by

$$I_s = max(M_{lmax}, M_{rep} * I_p). \tag{6}$$

This speed image is the maximum between the image of local maxima of the vesselness response, and the multiscale response multiplied by the probability image. The idea behind this expression is to prevent the centerline path to cross vessel contours and to find a path within another vessel or another structure. Thus the expression $M_{rep} * I_p$ will lower very fast close the vessel contours because of their high intensity local standard deviations. However, since small vessels could have a high local standard deviation almost everywhere, the possibility the possibility to cross them is preserved by the introduction of the local maxima of the vesselness response M_{lmax}.

2.3 Minimal-cost path, junction detection, and length checking

Two paths between the CCA and both the ECA and the ICA are automatically extracted maximizing the probability of being within and at the center of the searched vessel. As in [1], a geodesic distance transform is computed by the Fast Marching algorithm, starting from the end point up to the initial point. The extremities of both path are inputs of the semi-automatic challenge, and the speed function is set as the image I_s defined by equation 6, plus a small value of 0.02. The paths are created by backtracking the front evolution using the local intensity gradient of the geodesic distance. Once both paths have been detected, the junction point is defined as the point where the distance between the two paths becomes higher that 1mm, starting from their common extremity in the CCA. At the junction point, the path with higher value in Y axis is selected as the path to the ICA, and the other path is selected as the one to the ECA. This simple criterion has worked for all the datasets for which the junction has been successfully detected . Once the junction and both paths have been detected and identified, the path are either cut or extended depending on their actual distances to the detected junction and on the length requirements of the challenge. The extension of the paths is obtained by running another minimal cost path from the extremity to the targeted plane in Z coordinates.

3 Level Set Evolution

For each of the two paths detected previously, a level set segmentation method is used to evolve an active contour from the path to the vessel walls. The cylindrical tube around each path is create with a radius of 0.5mm. The level set evolution algorithm that we use is based on a previous publication [7]. The evolution force is composed of three main terms: a expansion term, an advection term and a smoothing term. As proposed by [8], the smoothing term is based on the minimal curvature of the active surface to better preserve small tubular structures. The advection term is based on the zero-crossing of the second order derivatives of the image intensity, and the expansion term is based on the following function of the image intensity: $e^{-\left(\frac{I(\mathbf{x})-\lambda_w}{2\sigma_w}\right)^2} - \tau$, where λ_w is an estimated mean intensity value of the vessel, σ_w is an estimated standard deviation of the vessel, and τ is a threshold that allows to shrink the surface (negative force), when the intensity of the current voxel is too far from the expected intensity. λ_w and σ_w are set as the mean and the standard deviation of the vessel intensity inside the initial tube, and τ is set to $e^{-2} \approx 0.135$ in all experiments. Figure 4 depicts surface rendering of the results obtained for datasets 000 and 004, together with isosurfaces of the corresponding ground-truths.

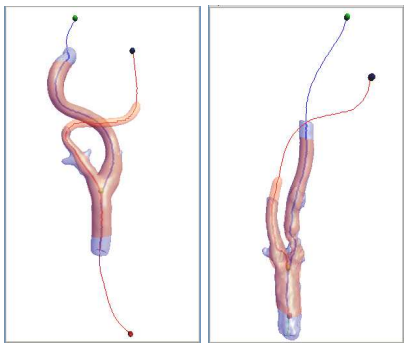

Figure 4: 3D representation of the initial points, the obtained paths, junctions, results and the given ground truth on datasets 000 (left) and 004 (right). The isosurfaces of the ground truth in red and the obtained level set results are displayed with transparency.

4 Results

Summary of the results obtained on the 31 testing datasets are given in tables 1 and 2. Even though the accuracy of the contours of the proposed method does not reach the expert precision, the method has been successful in detecting the paths and the junctions in most of the datasets. More difficulties have been encountered with the datasets from Hadassah and Louis Pradel, where in some cases, due to the importance of the calcifications or to the obstruction of the internal carotid artery, the junction has not been correctly detected and the full segmentation gives poor results since it relies strongly on the plane position of the junction to cut or expand the paths. Another important missing feature of the proposed method is to cut the unwanted branches, mainly appearing in the ECA, which would probably increase the quality of all the scores and would reduce the difference between the obtained results and the ones obtained by the experts. However, since the experts contribute to the generated ground truth, one can expect that their quantitative results are generally better than the one of the proposed technique.

Table 1: Summary lumen

Measure	**% / mm**			**rank**		
	min.	**max.**	**avg.**	**min.**	**max.**	**avg.**
L_dice	35.0%	95.6%	89.0%	1	4	3.68
L_msd	0.09mm	3.14mm	0.39mm	4	4	4.00
L_rmssd	0.12mm	4.51mm	0.64mm	4	4	4.00
L_max	0.33mm	12.20mm	2.66mm	1	4	3.77
Total (lumen)				**1**	**4**	**3.86**

Table 2: Averages lumen

Team name	**Total success**	**dice**		**msd**		**rmssd**		**max**		**Total rank**
		%	**rank**	**mm**	**rank**	**mm**	**rank**	**mm**	**rank**	
GIMET	31	89.0	3.7	0.39	4.0	0.64	4.0	2.66	3.8	3.9
ObserverA	31	95.4	1.5	0.10	1.5	0.13	1.6	0.56	2.0	1.6
ObserverB	31	94.8	2.5	0.11	2.4	0.15	2.3	0.59	1.8	2.2
ObserverC	31	94.7	2.4	0.11	2.1	0.15	2.1	0.71	2.5	2.3

5 Conclusion

A method has been described to segment the carotid bifurcation from Computed Tomography Angiography. The method is semi-automatic and requires three initial points, one in each of the main artery, to detect

first the centerline paths and the junction point between the external and the internal carotid arteries. In the proposed algorithm, the centerline paths are computed based on a multiscale vesselness response, and the contours are obtained by evolving a level set active contour from the centerline up to the vessel walls. The complete segmentation process presented in this paper is available within the opensource software AMILab at http://amilab.sourceforge.net/ , and the corresponding scripts will be available in the next release. As part of the MICCAI 2009 Challenge on Lumen Carotid Segmentation, experiments have been carried out on 15 training datasets and 31 testing datasets, where quantitative results are obtained for four different quality measures based on a ground truth obtained from three different experts. Results show that the proposed method behaves reasonably well, but without reaching the accuracy and the robustness of the experts. Future work will consists in improving the proposed method, by dealing better with branches and calcifications, and allowing a more adaptive expansion force that guides the level set active contour framework.

References

[1] T. Deschamps and L.D. Cohen. Fast extraction of minimal paths in 3d images and application to virtual endoscopy. *Medical Image Analysis*, 5(4), December 2001. 2.3

[2] G. Farnebäck. *Polynomial Expansion for Orientation and Motion Estimation*. PhD thesis, Linköping University, Sweden, SE-581 83 Linköping, Sweden, 2002. Dissertation No 790. 2.1

[3] K. Krissian, H. Bugunovic, J.M. Pozo, M.C. Villa-Uriol, and A. Frangi. Minimally interactive knowledge-based coronary tracking in cta using a minimal cost path. In *The MIDAS Journal - Grand Challenge Coronary Artery Tracking (MICCAI 2008 Workshop)*, September 2008. 2.1

[4] K. Krissian, J. Ellsmere, K. Vosburgh, R. Kikinis, and C.-F. Westin. Multiscale segmentation of the aorta in 3d ultrasound images. In *25th Annual Int. Conf. of the IEEE Engineering in Medicine and Biology Society (EMBS)*, pages 638–641, Cancun Mexico, September 2003. 2.1

[5] K. Krissian and G. Farnebäck. *Medical Imaging Systems Technology: Methods in Cardiovascular and Brain Systems*, chapter Techniques in the Enhancement of 3D Angiograms and their Applications, pages 359–396. World Scientific Publishing, 2005. 2.1

[6] K. Krissian, G. Malandain, N. Ayache, R. Vaillant, and Y. Trousset. Model based detection of tubular structures in 3d images. *Computer Vision and Image Understanding*, 80(2):130–171, nov 2000. 2.1, 2.1, 2.1

[7] K. Krissian and C.-F. Westin. Fast sub-voxel re-initialization of the distance map for level set methods. *Pattern Recognition Letters*, 26(10):1532–1542, 2005. 3

[8] L. M. Lorigo, O. D. Faugeras, W. E. L. Grimson, R. Keriven, R. Kikinis, A. Nabavi, and C.-F. Westin. Curves: Curve evolution for vessel segmentation. *Medical Image Analysis*, 5:195–206, 2001. 3